

OPTIMIZATON OF A MORPHING WING FOR RANGE

Durmuş Sinan Körpe¹
University of Turkish Aeronautical Association
Ankara, Turkey

Serkan Özgen²,
Middle East Technical University
Ankara, Turkey

ABSTRACT

In this study, an aerodynamic optimization tool is discussed. The computational tool involves a panel method, empirical relations for laminar and turbulent boundary layers in order to find the skin friction coefficient values (c_f) and a gradient based generalized reduced gradient method (GRGM). Result that is obtained with this tool is compared for three different wing configurations, i.e. original wing, optimized wing and a morphing wing for an experimental UAV. A rectangular baseline wing geometry is optimized for maximum range by varying its thickness and camber distribution at cruise speed (30 m/s) using spline method. Panel method is developed and validated with XFLR5, which is itself based on the panel method. Empirical laminar and turbulent skin friction coefficient formulas are used for parasite drag prediction. Michel's 1st formula is used for transition prediction. GRGM is developed and validated with a milestone problem in optimization studies. As a result of design process, it is found that 16.733% increase in aircraft range can be achieved compared to the original wing.

INTRODUCTION

Aviation adventure of human being was always inspired by the flight of birds. However, during the progress in aviation, wings of the birds cannot be mimicked due to lack of advanced materials and mechanisms. This situation brought the world into today's current aircraft configurations, which are designed and optimized for one or only a few flight conditions with fixed wing geometry, Figure 1. Contrary to this, due to success in advancing smart materials, including sensors, actuators, and their associated support hardware and micro-electronics, in recent years, there has been a growing interest in "morphing aircraft" which are defined at NASA Reports as the aircraft that are utilizing wings that have the capability to drastically change planform shape during flight – perhaps a 200% change in aspect ratio, 50% change in wing area, and a 20 degree change in wing sweep [Skillen and Crossley, 2007]. The ability of wing morphing promises the following improvements: improved performance covering the entire flight envelope, simplification of conventional control surfaces and their mechanisms, improvement of the quality of the flow field surrounding the vehicle which will result in drag reduction and lift increase, reduction of manufacturing costs, reduction of the vehicle empty weight, hence improved payload capacity and fuel economy. In this study, panel method and empirical formulas for laminar and turbulent boundary in order to find c_f are coupled with GRGM in order to define a minimization function and constraints for the optimization problem.

¹ Lecturer in Astronautical Engineering Department, Ph.D. Student in Aerospace Engineering Department at Middle East Technical University, Email: dskorpe@ae.metu.edu.tr

² Prof. in Aerospace Engineering Department, Email: sozgen@ae.metu.edu.tr

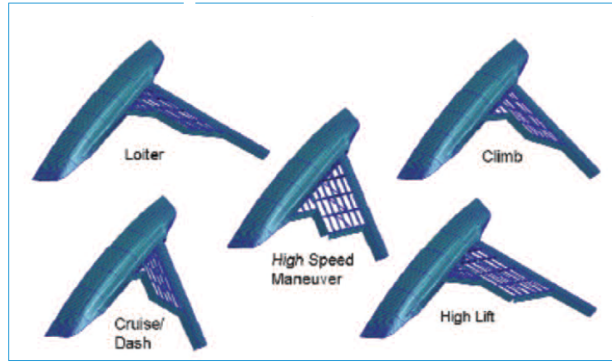


Figure 1: Wing configuration for different flight missions

METHOD

Panel Method

A panel method solver that has constant source and doublet distribution as singularity elements on each panel is developed. By using Dirichlet boundary condition, source strengths are fixed by using free stream potential and doublet strengths are remained as unknown. Kutta condition is satisfied by defining wake panels using the doublet strengths of the panels at trailing edge. With the help of the formulations in [Katz and Plotkin, 1991], a Fortran code (pan3d.f) was developed, which can model wing for different NACA airfoils, root chord (c_r), half span ($b/2$), taper ratio (λ), leading edge sweep angle (Λ), dihedral angle (Γ), incidence angle (θ) and twist angle (φ) values, and various tests were performed by comparing the results with XFLR5, whose prediction is in good agreement with the experimental results [Deperrois, 2008]. Comparison of pan3d.f results with XFLR5 in terms of pressure distribution is illustrated in Figure 2, while the comparisons of lift coefficient (C_L) and induced drag coefficient (C_{Di}) for half wing, can be seen in Table 1. For these results density and velocity are taken as 1.225 kg/m^3 and 30 m/s , respectively.

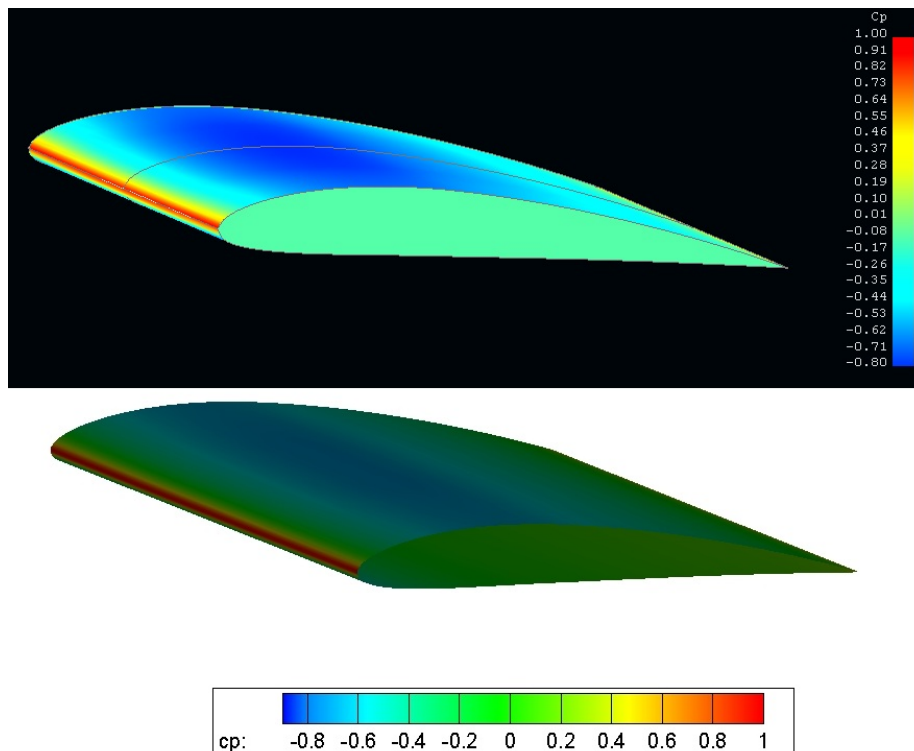


Figure 2: Wing geometry from XFLR5 (top), pan3d.f (bottom) (NACA 4412, $c_r = 0.4 \text{ m.}$, $b/2 = 1.5 \text{ m.}$, $\lambda = \Lambda = \Gamma = \theta = \varphi = 0$)

Table 1: C_L and C_{Di} results for pan3d.f and XFLR5 for different α (NACA 4412, $c_r = 0.4$ m., $b/2 = 1.5$ m., $\lambda = \Lambda = \Gamma = \theta = \varphi = 0$)

angle of attack (α)	pan3d.f		XFLR5	
	C_L	C_{Di}	C_L	C_{Di}
0	0,4104	0,0059	0,4191	0,006
2	0,5993	0,01728	0,6033	0,01553
4	0,7881	0,02032	0,7904	0,02183
6	0,9732	0,03105	0,9812	0,03224
8	1,1569	0,04393	1,1593	0,04678

As it is seen in Table 1, pan3d.f results matches very well with the results of XFLR5 for different angle of attacks. But it is obvious that pand3d.f is a very useful tool as a fast aerodynamic solver.

Boundary Layer Solver

A simple boundary layer solver is implemented into the design tool by using the methodology below [Moran, 1984];

1. Find stagnation point at each spanwise strip,
2. For stagnation point, use the formula below for momentum thickness (θ),

$$\theta(0) = \frac{0.075 * \rho}{\mu \frac{dV}{dx}} \quad 1$$

3. For laminar region, use the formula below for momentum thickness and c_f ,

$$\theta = \frac{0.73 * x}{\sqrt{Re_x}} \quad 2$$

$$c_f = \frac{0.73}{\sqrt{Re_x}} \quad 3$$

4. Use Michel's 1st formula for transition from laminar to turbulence prediction,

$$Re_\theta = 1.174 * \left(1 + \frac{22400}{Re_x}\right) * Re_x^{0.46} \quad 4$$

5. For turbulent region, use the formula for c_f ,

$$c_f = \frac{0.074}{Re_x^{0.2}} \quad 5$$

After this methodology, boundary layer calculations from stagnation point to trailing edge over upper and lower surfaces can be accomplished.

GRGM

GRGM is developed by using Fortran [Ravindran, Ragsdell and Reklaitis, 2006] [Rao, 2009] and tested by following optimization problem for minimum material volume in a structural design under load [Vanderplaats, 2007]. In order to develop a user-friendly solver, basic constraint consensus algorithm that is used for moving from infeasible to feasible direction is implemented into the solver [Ibrahim and Chinneck, 2008]. The design parameters are the width (b) and height (h) at each of the N segment, where N=5. It is asked to find the minimum weight of the system whereas stress (σ) at left hand of each segment is less than 14000 N/cm² and tip deflection (y) under load is less than 2.5 cm.

The geometrical requirements are the height of any segment does not exceed twenty times the width for each segment. Figure 3 shows the design variables on the beams segments. Each segment has a length of 100 cm and 50000 N force applied at the end of fifth segment. Equation 6 is a mathematical representation of the problem.

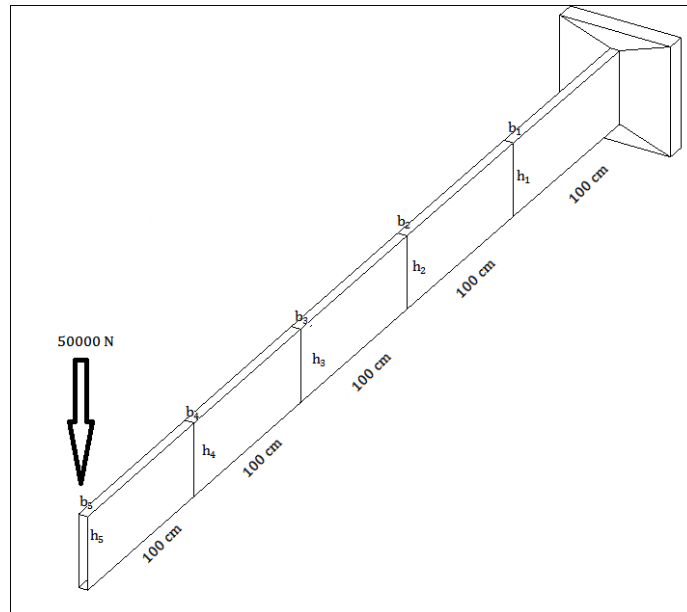


Figure 3: *Cantilever beam*

$$\begin{aligned} & \text{Min} \sum_{i=1}^5 V_i \\ & \sigma_i - 14000 \leq 0 \quad i = 1, N \\ & h_i - 20b_i \leq 0 \quad i = 1, N \\ & y_N - 2.5 \leq 0 \\ & b_i \geq 1 \quad i = 1, N \\ & h_i \geq 5 \quad i = 1, N \end{aligned}$$

6

The algorithm that is developed by generalized reduced gradient method is compared with the following methods:

1. Genetic search of EVOLVE software,
2. Sequential linear programming of DOT optimization software contained in the visualDOC PROGRAM,
3. Method of feasible directions of ADS research program,
4. Generalized reduced gradient method of ADS research program,
5. Modified feasible directions method of DOT optimization software contained in the visualDOC PROGRAM,
6. Sequential quadratic programming of DOT optimization software contained in the visualDOC PROGRAM,
7. Developed GRGM.

As it is seen in Table 2, the developed program, Method 7, obtains the optimum value when it is compared with other methods. Moreover, when the problem related with finding feasible region algorithm in GRGM is solved, its iteration value is expected to decrease at least one step when it is compared with Method 4, which is another generalized reduced gradient method.

Table 2: *Iteration history of the methods in cm³*

Iteration number	Methods						
	1*	2	3	4	5	6	7
0	0	100000	100000	100000	100000	100000	100000
1	56680	60805	106425	104500	110735	88901	130840
2	56680	59351	111014	95849	88454	69929	107326
3	56.60	64753	92922	93329	80427	64284	94321
4	71570	64732	82511	76763	71711	64628	81425
5	71570	64097	73805	68960	69500	64694	78546
6	71590	64418	70683	67445	67843	65480	73454
7	71590	64294	69540	65898	67636	65436	71221
8	66880	64519	68133	65814	66362	65427	68543
9	66880	64434	66830	65422	65426	-	66716
10	66880	65530	65906	65399	65425	-	65860
11	66880	65493	65906	65399	65425	-	65590
Iterations	6667	12	18	11	11	8	12

RESULT AND DISCUSSION

The experimental UAV can be seen in Figure 4. For the UAV, there are 3 wing configurations. The 1st one, original wing (OrW), is a rectangular wing that has a Wortmann FX 63–137 airfoil with 0.33 m. chord and 2.4 m. span. The aim of the wing was to carry 100 N in level flight. For second and third wing configuration, optimization technique is applied at which the airfoil shape is same along span and it is obtained by using splines.



Figure 4: *Experimental UAV [Gamboa, Vale, Lau and Suleman, 2009]*

The second wing configuration, optimized wing (OpW), is obtained by using the following optimization problem in Equation 7, which has only one equality constraint for 30 m/s cruise speed. The initial airfoil for this design is SD-2030.

$$\begin{aligned}
& \text{Min } C_D @ V_\infty = 30 \text{ m/s} \\
& L = W \\
& 0.1 \leq c_r, c_t \leq 0.33 \\
& 2 \leq b \leq 3.4 \\
& -4 \leq \theta \leq 0 \\
& -5 \leq \alpha \leq 15 \\
& v_6 \geq 0.01 \\
& v_i \geq 5 \quad i = 7, 11
\end{aligned}$$

7

In Equation 7, v values are spline control points, which create a sequence shape that is followed by spline closely as it is seen in Figure 5.

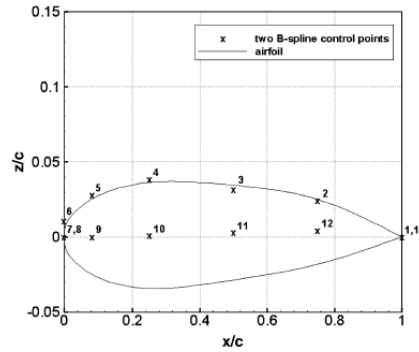


Figure 5: Control points for thickness and camber distribution and resulting airfoil geometry [Gamboa, Vale, Lau and Suleman, 2009]

For 2nd and 3rd wing configuration, which is morphing wing (MW), empirical weight formulation is used in order to take into account of change in weight of horizontal tail, vertical tail and wing due to change in wing area, taper ratio, aspect ratio, etc. The 3rd wing configuration, MW, is obtained by using the optimization problem in Equation 8, which has 1 equality and 20 inequality constraint. The initial airfoil is NACA 0009.

$$\begin{aligned}
& \text{Min } C_D @ V_\infty = 30 \text{ m/s} \\
& L = W \\
& 0.22 \leq c_r, c_t \leq 0.33 \\
& 2.4 \leq b \leq 3.4 \\
& 4 * 10^{-3} \leq \left| Z_{\frac{x}{c}=0.75} \right| \leq 7.2 * 10^{-3} \\
& 6 * 10^{-3} \leq \left| Z_{\frac{x}{c}=0.5} \right| \leq 10.8 * 10^{-3} \\
& 7 * 10^{-3} \leq \left| Z_{\frac{x}{c}=0.25} \right| \leq 12.6 * 10^{-3} \\
& 6 * 10^{-3} \leq \left| Z_{\frac{x}{c}=0.167} \right| \leq 10.8 * 10^{-3} \\
& 5.5 * 10^{-3} \leq \left| Z_{\frac{x}{c}=0.083} \right| \leq 9.9 * 10^{-3}
\end{aligned}$$

8

The inequality constraints are used in order to define maximum and minimum thickness values for upper and lower part of the airfoil at 75%, 50%, 25%, 16.7% and 8.3% percent of the chord. Due to physical limitation in morphing mechanism, a fixed leading edge diameter, $4 * 10^{-3}$ m., is imposed to the optimization problem.

In order to test aerodynamic optimization tool, an optimization problem is chosen which is very similar to the problem defined in Equation 8. In this optimization problem, morphing mechanism is only used in order to change thickness and camber shape of the wing (TCW). In addition to this, empirical weight formula is not applied and W is taken as 106.1 N, which is the final weight that is obtained at the end of optimization problem solution for OpW. NACA 0009 is also initial airfoil for this design.

Figure 6 depicts the airfoils for these 4 different wing configurations.

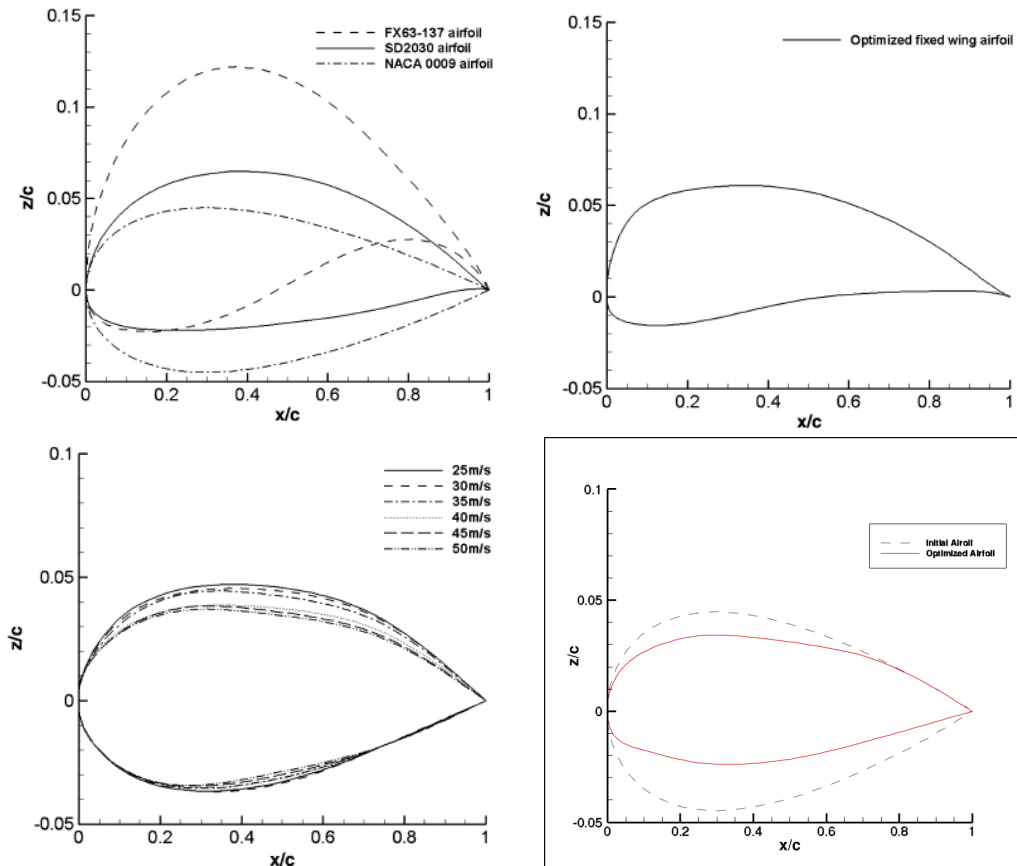


Figure 6: OrW (top left, dashed airfoil), OpW (top right), MW (bottom left, dashed airfoil) and TCW (bottom right)

The results in Table 3 show the corresponding weight, wing drag (D_W), C_L/C_D , $\ln(W_0/W_1)$ and range improvement with respect to OrW for 4 different wing configurations. In this study, it is aimed to find the longest range at cruise speed (30 m/s) for the UAV with original wing. Results are obtained by using historical Breguet formula and it is assumed that UAV takes off with 10 N. of fuel and consumes all of the fuel for range mission at 30 m/s. For MW, there is no information related with its final weight. Therefore, it is assumed as 106.1 N.

Table 3: Results for 4 different wing configurations

Wing	Weight (N)	Wing Drag (N)	C_L/C_D	$\ln(W_0/W_1)$	Improvement in Range (%)
OrW	100	5.8	6.881	0.105	0.0
OpW	106.1	2.6	9.366	0.099	27.874
MW	106.1	2.7	9.281	0.099	26.720
TCW	106.1	3.678	8.550	0.099	16.733

One of the key parameter in evaluation of drag reduction is the comparison of range values. As it seen from Table 3, TCW provides an advantage of 16.733% when it is compared with OrW. As it is predicted, OpW and MW are more effective wings for Range. OpW yields better results, because it is the fully optimized wing for 30 m/s. However, it is very important to see the fact that more morphable

systems require more complexity, which yields more empty weight. When this fact is kept in view, morphing system that is designed for just for thickness and camber variation is a good compromise.

FUTURE WORK

The aerodynamic design tool will be developed by implementation of solvers for momentum, energy thickness for both laminar boundary layer and turbulent boundary layer. It is planned to use wake modeling method for separation. After this implementation, it is expected to find the best range for TCW by defining free stream velocity to the optimization problem.

References

Gamboa P., Vale J., Lau F. J. P. and Suleman A. (2009), *Optimization of a Morphing Wing Based on Coupled Aerodynamic and Structural Constraints*, AIAA J., V. 44, No. 9, p. 2087-2104.

Rao S. S. (2009), *Engineering Optimization: Theory and Practice*, John Wiley & Sons, Inc..

Ibrahim W. and Chinneck J. W. (2008), *Improving Solver Success in Reaching Feasibility for Sets of Nonlinear Constraints*, Computers and Operations Research, Vol. 35, pp. 1394-1411.

Deperrois, A. (2008), *Results vs. Prediction*, Presentation document.

Vanderplaats, G. N. (2007), *Multidiscipline Design Optimization*, Vanderplaats Research and Development Inc., p: 152-197.

Skillen, M. D. and Crossley, A. (2007), *Modeling and Optimization for Morphing Wing Concept Generation*, NASA/CR - 2007-214860.

Ravindran A., Ragsdell K. M. and Reklaitis G. V. (2006), *Engineering Optimization: Methods and Applications*, John Wiley & Sons, Inc..

Katz, J. and Plotkin, A. (1991), *Low-speed Aerodynamics: From Wing Theory to Panel Methods*, McGraw-Hill.

Moran, J. (1984), *An Introduction to Theoretical and Computational Aerodynamics*, John Wiley & Sons Inc., p: 191-260.